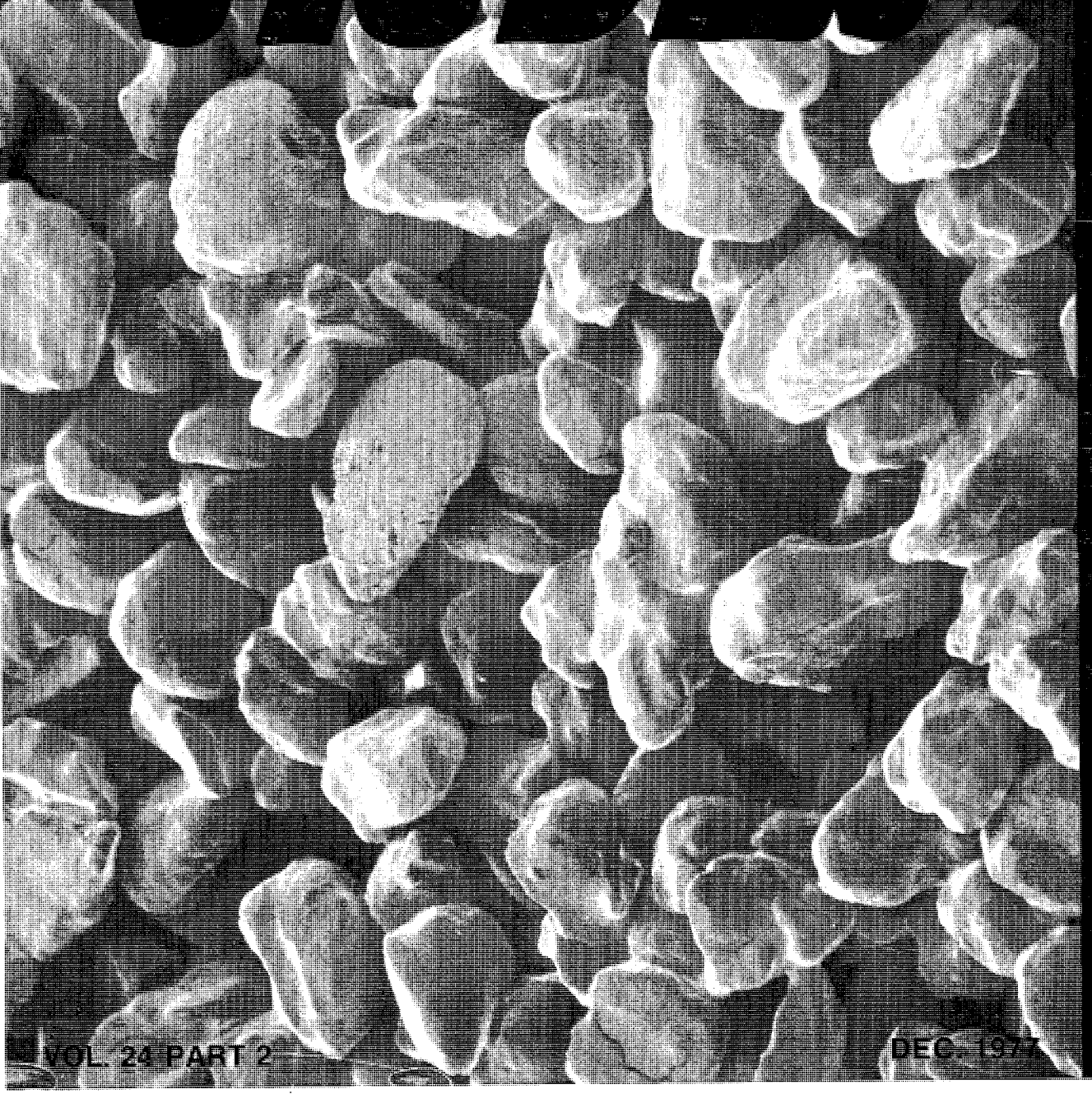


# GEOLOGY STUDIES



VOL. 24 PART 2

DEC. 1977



# Brigham Young University Geology Studies

## Volume 24, Part 2

### CONTENTS

Studies for Students: A Question Set for Sands and Sandstones .....	Sedimentation Seminar
A New Species of <i>Arroyocrinus</i> (Inadunata) from the Park City Formation (Upper Permian) of Utah .....	H. L. Strimple and J. F. Miller
Additional Specimens of the Hypsilophodontid Dinosaur <i>Dryosaurus altus</i> from the Upper Jurassic of Western North America .....	Jeffrey D. Shepherd, Peter M. Galton, and James A. Jensen
Paleoenvironments of the Moenave Formation, St. George, Utah .....	John Daniel Davis
Foraminiferal Abundance Related to Bentonitic Ash Beds in the Tununk Member of the Mancos Shale (Cretaceous) in Southeastern Utah .....	Rebecca Lillywhite Bagshaw
Paleoecology of the Lower Carmel Formation of the San Rafael Swell, Emery County, Utah .....	Lawrence H. Bagshaw
Structure, Stratigraphy, and Tectonic History of the Indianola Quadrangle, Central Utah .....	David M. Runyon
Compound Faceted Spurs and Recurrent Movement in the Wasatch Fault Zone, North Central Utah .....	Thomas C. Anderson
A Subsurface Correlation of Permian-Triassic Strata in Lisbon Valley, Utah .....	Ralph T. Bohn
Mesozoic-Cenozoic Structural Development of the Kern Mountains, Eastern Nevada-Western Utah .....	Robert C. Ahlborn

Publications and Maps of the Geology Department



Cover: Sahara dune sand, X130. Photo courtesy Amoco Production Research, Tulsa, Oklahoma, contributed by Paul E. Potter, Department of Geology, University of Cincinnati, Cincinnati, Ohio 45221.

A publication of the  
Department of Geology  
Brigham Young University  
Provo, Utah 84602

Editors

W. Kenneth Hamblin  
Cynthia M. Gardner

*Brigham Young University Geology Studies* is published semiannually by the department. *Geology Studies* consists of graduate-student and staff research in the department and occasional papers from other contributors. *Studies for Students* supplements the regular issues and is intended as a series of short papers of general interest which may serve as guides to the geology of Utah for beginning students and laymen.

ISSN 0068-1016

Distributed December 1977

Price \$5.00

(Subject to change without notice)

12-77 525 28856

## CONTENTS

STUDIES FOR STUDENTS: A QUESTION SET FOR SANDS AND SANDSTONES .....	1	PALEOENVIRONMENTS OF THE MOENAVE FORMATION, ST. GEORGE, UTAH .....	17
I. Questions primarily answered in the laboratory .....	1	Introduction .....	17
II. Questions primarily answered by the megascopic examination of outcrops and cores and by the study of wire line logs .....	4	Previous work .....	17
III. Format for a basin—Questions primarily answered by study of the entire basin or perhaps even a larger area such as a continental margin .....	6	Location .....	18
Figures .....		Methods of study .....	18
1. Definition sketch of a typical sandstone .....	2	Acknowledgments .....	18
2. Minerals filling sandstone interstices .....	3	Geologic setting .....	19
3. Flow chart using wire line logs .....	5	General sedimentary features .....	19
4. Flow chart for basin analysis .....	6	Geometry .....	21
Tables .....		Channel-filling mechanisms .....	21
1. Classification of sand and sandstone bodies .....	4	Composition .....	23
2. Format for basin study: properties and methods .....	7	Sedimentary structures .....	23
A NEW SPECIES OF <i>ARROYOCRINUS</i> (INADUNATA) FROM THE PARK CITY FORMATION (UPPER PERMIAN) OF UTAH .....	9	Paleocurrent data .....	24
Introduction .....	9	Fossils .....	26
Systematic paleontology .....	9	Interpretation and reconstruction of the Moenave environment of deposition .....	27
Description .....	9	Interpretation I .....	27
Discussion .....	9	Interpretation II .....	28
Measurements of holotype in millimeters .....	10	Reconstruction of the Moenave tidal flat environment .....	29
Occurrence .....	10	Summary .....	30
Holotype .....	10	References cited .....	30
Acknowledgments .....	10	Figures .....	
References .....	10	1. Index map .....	18
Figures .....		2. Moenave Formation stratigraphy .....	19
1. Photographs .....	9	3. North channel in airport roadcut .....	20
2. Camera lucida drawings .....	10	4. South channel in airport roadcut .....	20
ADDITIONAL SPECIMENS OF THE HYPHILOPHODONTID DINOSAUR <i>DRYOSAURUS ALTUS</i> FROM THE UPPER JURASSIC OF WESTERN NORTH AMERICA .....	11	5. Schematic drawing of tabular appearance of massive mudstone layers which enclose the channel deposits .....	20
Introduction .....	11	6. Bedding plane inclinations in channels .....	21
Data on specimens .....	11	7. Bundles of ribbon sand bodies at Interstate 15 roadcut .....	22
Acknowledgments .....	11	8. Schematic drawing of ribbon sand bodies, Interstate 15 roadcut .....	22
Description and comparisons .....	11	9. Intraformational conglomerate lens .....	23
Vertebral column .....	11	10. Flaser bedding .....	23
Pectoral girdle .....	12	11. Wavy bedding .....	23
Fore limb .....	12	12. Planar cross-bedding .....	24
Pelvic girdle .....	12	13. Small-scale trough type cross-bedding .....	24
Hind limb .....	13	14. Paleocurrent trends in channel undulations .....	24
Discussion .....	14	15. Vector diagrams of paleocurrent trends .....	25
References cited .....	15	16. Location map of paleocurrent measurements along the erosional cliffs north of St. George Blvd. ....	26
Figures .....		17. Location map of paleocurrent measurements for positions G and H .....	26
1. Vertebrae .....	12	18. Paleocurrent summary diagram of positions A-J .....	27
2. Pectoral girdle and forelimb .....	13	19. Vertical burrows .....	28
3. Pelvic girdle .....	13	20. Horizontal burrows .....	28
4. Femora and tibiae .....	14	21. Burrows preserved as cavities .....	28
5. Pes .....	15	22. Reconstructed model diagram of the Moenave tidal flat in the St. George area .....	29
		23. Regional paleocurrent trends .....	30
		Table .....	
		1. Summary of current flow data .....	25
		FORAMINIFERAL ABUNDANCE RELATED TO BENTONITIC ASH BEDS IN THE TUNUNK	

# MEMBER OF THE MANCOS SHALE (CRETACEOUS) IN SOUTHEASTERN UTAH

Introduction .....	33
Acknowledgments .....	33
Previous work .....	33
Field and laboratory methods .....	34
Fauna .....	34
Paleoecology .....	35
Conclusions .....	39
Systematic paleontology .....	39
References cited .....	48
Figures .....	
1. Stratigraphic section .....	33
2. Index map .....	34
3. View of Tununk stratigraphy .....	35
4. View of trench through ash 2 .....	35
5. Graph of foraminiferal abundance in ash 1 .....	36
6. Graph of foraminiferal abundance in ash 2 .....	37
7. Graph of foraminiferal abundance in ash 3 .....	38
8. Graph of foraminiferal abundance in ash 4 .....	39
9. Graph of foraminiferal abundance in ash 5 .....	40
10. Foraminiferal fauna .....	42
11. Foraminiferal fauna .....	44
12. Foraminiferal fauna .....	46
13. Foraminiferal fauna .....	47
Tables .....	
1. Foraminiferal occurrence in ash 1 .....	36
2. Foraminiferal occurrence in ash 2 .....	37
3. Foraminiferal occurrence in ash 3 .....	38
4. Foraminiferal occurrence in ash 4 .....	39
5. Foraminiferal occurrence in ash 5 .....	41

# PALEOECOLOGY OF THE LOWER CARMEL FORMATION OF THE SAN RAFAEL SWELL, EMERY COUNTY, UTAH

Introduction .....	51
Acknowledgments .....	51
Location .....	51
Methods of study .....	51
Previous work .....	52
Geologic setting .....	52
Lithologies .....	53
Sandstone .....	53
Light yellow brown sandstone .....	53
Medium brown sandstone .....	53
Siltstone .....	53
Red siltstone .....	53
Gypsiferous and dolomitic siltstone .....	55
Shale .....	55
Green shale .....	55
Grey shale .....	55
Red shale .....	55
Carbonate rocks .....	55
Calcarenite .....	56
Dololutite .....	56
Dolarenite .....	56
Sedimentary structures .....	56
Ripple marks .....	56
Flute casts .....	57
Mudcracks .....	57
Miscellaneous .....	57
Paleontology .....	57
Faunal assemblages .....	57

Autecology .....	59
<i>Trigonia</i> and <i>Vaugonia</i> .....	
<i>Camptonectes</i> .....	
<i>Gryphea</i> (?) .....	
<i>Modiolus</i> (?) and <i>Nucula</i> (?) .....	
Environment .....	59
General .....	59
Salinity .....	59
Temperature .....	59
Interpretation of sedimentary environments .....	59
Tidal flat .....	59
Open marine .....	60
Barrier lagoon .....	60
Sedimentary model .....	60
Conclusions .....	61
Appendix .....	61
References cited .....	62
Figures .....	
1. Index map .....	51
2. Stratigraphic section .....	52
3. Generalized east-west Carmel time cross section .....	53
4. Paleogeographic setting of the study area .....	53
5. Field views .....	54
6. Photomicrographs .....	55
7. Stratigraphic section .....	56
8. Fossils and an unusual sedimentary structure .....	58
9. Sedimentary model .....	60

# STRUCTURE, STRATIGRAPHY, AND TECTONIC HISTORY OF THE INDIANOLA QUADRANGLE, CENTRAL UTAH

Introduction .....	63
Acknowledgments .....	63
Previous work .....	63
Geologic evolution and regional setting .....	64
Present-day setting .....	65
Stratigraphy .....	65
Jurassic .....	66
Arapien Shale .....	66
Twist Gulch Formation .....	67
Cretaceous .....	67
Indianola Group .....	67
South Flat Formation .....	68
Price River Formation .....	69
Cretaceous-Tertiary .....	70
North Horn Formation .....	70
Tertiary .....	71
Flagstaff Formation .....	71
Green River Formation .....	72
Unnamed volcanic rocks .....	73
Quaternary .....	74
Unnamed .....	74
Sedimentary tectonics .....	75
Structure .....	76
Faults .....	76
Joints .....	78
Folds .....	78
Tectonic history .....	78
Economic geology .....	79
Overview .....	79
Appendix .....	80
Arapien Formation .....	80
Twist Gulch Formation .....	80
Indianola?-Price River Formation? .....	81

North Horn Formation .....	81
Flagstaff Formation .....	81
References cited .....	81
Figures .....	
1. Index map .....	65
2. Stratigraphic column .....	65
3. Hjork Creek diapir (Twist Gulch) .....	66
4. North San Pitch collapsed diapir (high altitude vertical) .....	66
5. Hjork Creek vertical outcrop .....	68
6. Price River outcrop, overturned South Flat .....	69
7. Formline contour map .....	69
8. North Horn channels .....	71
9. North Horn "giant" algal balls .....	71
10. North Horn algal ball .....	71
11. Pollen photomicrographs .....	73
12. Tertiary volcanic stream deposits .....	74
13. North San Pitch collapsed diapir (low oblique) ....	75
14. Salt Valley cuesta .....	75
15. Green River cuesta .....	75
16. Seven-step geologic evolution .....	76
17. Stream pattern analysis. Stippled areas denote areas of controlled drainage .....	77
18. Rebound diagram .....	79
19. Geologic map with cross sections A-A', B-B', and C-C' .....	in pocket

# COMPOUND FACETED SPURS AND RECURRENT MOVEMENT IN THE WASATCH FAULT ZONE, NORTH CENTRAL UTAH .....

Introduction .....	83
Acknowledgments .....	83
Previous studies .....	83
Early work .....	83
General geology .....	84
Wasatch fault geometry .....	85
Geophysics .....	86
Origin of pediments .....	86
Conceptual model .....	86
Pediment formation .....	86
Recurrent uplift .....	88
Pediment preservation .....	88
Downcutting .....	88
Slope retreat .....	89
Structural control .....	89
Sequential development .....	89
Methods .....	89
Aerial photography .....	90
Pediment mapping .....	90
Profile projection .....	91
Correlation .....	91
Results .....	93
Payson Canyon to Spanish Fork Canyon .....	95
Spanish Fork Canyon to Springville .....	95
Springville to Provo Canyon .....	95
Provo Canyon to American Fork Canyon .....	95
American Fork Canyon to the Traverse Mountains ....	96
Conclusions .....	97
Pediment formation and slope retreat .....	97
Uplift and quiescence .....	97
Absolute dating .....	99
Tilt .....	99
Regional geodynamics .....	99
Suggested further studies .....	99

References cited .....	99
Figures .....	
1. Index map .....	84
2. Conceptual model of compound faceted spur development .....	87
3. Spanish Fork Peak .....	90
4. Selected facets on Spanish Fork Peak .....	90
5. Area near Hobbie Creek Canyon .....	90
6. Section of Spanish Fork Peak quadrangle topographic map .....	91
7. Same map as figure 6 with facets and pediments identified .....	91
8. Profile of rangefront .....	92
9. Loafer Mountain area with key pediment correlations .....	94
10. Spanish Fork Peak area with key pediment correlations .....	94
11. Hobbie Creek area with key pediment correlations .....	94
12. Maple Flat area with key pediment correlations ....	95
13. Mount Timpanogos area with key pediment correlations .....	96
14. Alpine area with key pediment correlations .....	96
15. Stranded streams at Corner Creek area .....	97
16. Generalized profile of range showing main correlations and uplift patterns .....	97
17. Sketches of the Spanish Fork Peak area showing probable historical development .....	98

# A SUBSURFACE CORRELATION OF PERMIAN-TRIASSIC STRATA IN LISBON VALLEY, UTAH ....

Introduction .....	103
Acknowledgments .....	103
Previous work .....	103
Geologic setting .....	103
Stratigraphy .....	103
Structure .....	107
Cutler stratigraphy .....	107
Sandstones .....	107
Calcareous arkose .....	107
Arkosic wacke .....	107
Mudstones .....	108
Sandy mudstone .....	108
Mudstone .....	108
Sandy limestone .....	109
Chinle stratigraphy .....	109
Sandstone .....	109
Calcareous arkose .....	109
Arkosic wacke .....	109
Mudstone .....	109
Sandy mudstone .....	109
Mudstone .....	110
Conglomerate .....	110
Mudstone conglomerate .....	110
Stratigraphic correlation .....	111
Appendix .....	113
Measured section .....	113
Core 3 .....	114
Core 9 .....	115
References cited .....	115
Figures .....	
1. Index map .....	104
2. Fence diagram .....	105
3. Map of Lisbon Valley .....	106

4. Stratigraphic column .....	106	General statement .....	123
5. Cutler Formation calcareous arkose .....	107	Metamorphic rocks .....	125
6. Cutler Formation arkosic wacke .....	108	General statement .....	125
7. Mudstone .....	108	Metamorphic rock description .....	125
8. Cutler Formation sandy limestone .....	109	Marble and dolomarlle .....	125
9. Diagram of cores .....	110	Phyllitic rocks .....	126
10. Chinle Formation calcareous arkose .....	111	Calc-silicate rocks .....	126
11. Chinle Formation arkosic wacke .....	111	Schist .....	126
12. Chinle Formation conglomerate .....	112	Quartzite .....	126
13. Cutler and Chinle formations .....	112	Metagneous rocks .....	126
Tables .....		Mineral assemblages .....	126
1. Logs and drilling data .....	104	Mafic assemblages .....	126
2. Core composition .....	106	Pelitic assemblages .....	126
		Calcareous and calc-silicate assemblages .....	127
MESOZOIC-CENOZOIC STRUCTURAL DEVELOPMENT OF THE KERN MOUNTAINS, EASTERN NEVADA-WESTERN UTAH .....	117	Contact vs. regional metamorphism .....	127
Introduction .....	117	Age of metamorphic rocks .....	127
Previous work .....	117	Igneous rocks .....	128
Acknowledgments .....	117	General statement .....	128
Structures of the sedimentary cover .....	117	Volcanic rocks .....	128
General statement .....	117	Rhyodacite .....	128
Low-angle faults .....	118	Dacitic rocks .....	129
Regional denudation .....	119	Tuff .....	129
Local denudation .....	119	Summary and conclusions .....	129
High-angle faults .....	120	References cited .....	130
Folds .....	120	Figures .....	
Metamorphic structures .....	121	1. Index map .....	118
General statement .....	121	2. Structural outline .....	119
Skinner Canyon study .....	121	3. Geologic map .....	in pocket
Macroscopic structures .....	121	4. Sterographic projection of fold axes .....	121
Mesoscopic fabric .....	121	5. Sterographic projection of axial planes .....	121
Microscopic fabric .....	122	6. Sterographic projection of metamorphic foliation .....	121
Structure of the plutonic complex .....	122	7. Sterographic projection of granitic foliation .....	123
General statement .....	122	8. Sterographic projection of joints .....	123
Foliation .....	122	9. Sterographic projection of aplitic dikes .....	123
Joints .....	123	10. Generalized stratigraphic column of regional stratigraphic and Kern Mountains stratigraphic column .....	124
Dikes .....	123	11. Generalized geologic map of Kern Mountains .....	125
Stratigraphy .....	123	12. Metamorphic rock correlation .....	129
		Table .....	
		1. Kern Mountains geologic history .....	120



# A Subsurface Correlation of Permian-Triassic Strata in Lisbon Valley, Utah\*

RALPH T. BOHN  
*Getty Oil Co., Denver, Colorado 80202*

**ABSTRACT.**—The uppermost part of the Permian age Cutler Formation and the lower part of the Moss Back Member of the Chinle Formation were examined with the use of cores and outcrop in the area of Lisbon Valley, Utah. Nine cores and one outcrop section were used to evaluate facies changes in the Cutler Formation and Moss Back Member of the Chinle Formation. Cores and outcrop data were also used to describe the unconformity separating the two units. Facies in the Moss Back Member of the Chinle Formation are conglomerate, mudstone, arkosic wacke, and calcareous arkose. These facies occur as relatively thin units that tend to be laterally extensive and grade upward from one to another. The uppermost part of the Cutler Formation appears to be composed of thick beds of sandstone and mudstone that are laterally extensive. The unconformity separating the Cutler Formation and the Moss Back Member of the Chinle Formation appears to represent a time of nondeposition with no erosion or subaerial exposure.

## INTRODUCTION

This study deals with Permian-Triassic rocks in the subsurface and surface outcrop in the area of Lisbon Valley, located about 48 km south of Moab in San Juan County, Utah (fig. 1).

I propose, through the data presented in this study, to give an interpretation and description of the facies changes between cores and outcrop in the Lisbon Valley area. I will also describe the unconformity separating Permian and Triassic strata in the study area. This study of facies correlations (fig. 2) was done using hand-sample descriptions (appendix), and thin-section studies. Standard stains and faunal analysis were also used as tools in interpretation. Data were gathered from both cores and outcrops. Cores were obtained from Amerada Petroleum Corporation. Wells from which cores were used are located in sections 17, 20, 25, and 26, T. 29 S, R. 24 E; section 31, T. 29 S, R. 25 E; and section 5, T. 30 S, R. 25 E (fig. 1). The outcrop section is located in sections 12 and 13, T. 30 S, R. 25 E (fig. 1). Amerada Petroleum Corporation has also provided logs and drilling data, a list of which can be found in table 1.

## Acknowledgments

I would like to thank Amerada Petroleum Corporation for providing the cores and logs used in this study. I am indebted to many people who have given me help, particularly Dr. James L. Baer for his advice and comments throughout its preparation. Special thanks are extended to my parents, without whom I would have been unable to complete my work. I would also like to give special thanks to my wife for her help in preparing illustrations, typing, and giving me encouragement.

## Previous Work

Geologic work in Lisbon Valley has been carried out as a part of general geologic investigations of the Colorado Plateau and Paradox Basin. The history of geologic investigation of the Chinle Formation is documented by Stewart et al. (1972). The first major surveys were conducted from 1860 to 1890 by Wheeler, Hayden, King, and Powell.

Powell recognized four major groups in the Triassic and Jurassic, one of which was the Shinarump Group which included what has now been defined as the Chinle Formation. The Chinle Formation and its four members were formally named and defined in the period from the Powell survey to 1920. Uranium exploration from 1950 to the early 1960s brought a flurry of geologic activity in the Colorado Plateau and in Lisbon Valley. During this time many studies were undertaken to define the stratigraphic relationships of uranium-bearing formations. Mesozoic formations exposed in Lisbon Valley were mapped by Weir et al. (1955a, 1955b, 1956, 1957a, 1957b, 1958, and 1959).

## GEOLOGIC SETTING

Lisbon Valley lies in the central part of the Paradox Basin (fig. 3) within the Colorado Plateau physiographic province. The formations that crop out in this area range in age from Permian to Cretaceous (Weir and Puffett 1958; Lekas and Dahl 1956).

## Stratigraphy

Stratigraphy of the lower Paleozoic and Precambrian in the Paradox Basin is not well documented because of the limited subsurface control. Precambrian rocks are igneous and metamorphic. Cambrian was a time of marine transgressions over the Precambrian surface. Deposits of this period were beach sands, laid down by the advancing sea, and shelf carbonates. Ordovician- and Silurian-age rocks are not preserved in the Paradox Basin area. Lack of these rocks documents a period of regression and regional uplift. Late Devonian and Mississippian history was similar to Cambrian history and documents another transgression of the sea. A period of erosion ended the Mississippian and signified the start of a new tectonic regime.

Formation of the Paradox Basin began in early Desmoinesian time. The major uplift shedding clastics into the basin was the Uncompahgre-San Luis uplift. Of lesser importance were the Emery, Kaibab, and Zuni-Defiance uplifts (fig. 3). All were part of the ancestral Rocky Mountain orogeny. The present Uncompahgre uplift is a fault-bounded block cored by Precambrian and igneous rocks. Vertical faults with more than 6,150 m displacement, as indicated by the clastic wedge on its flanks, bound the Uncompahgre.

Sediments in the Paradox Basin generally thicken towards the Uncompahgre Uplift and thin to shelf carbonates toward the other uplifts of Pennsylvanian time. The oldest formation of Pennsylvanian age in the Paradox Basin is the Molas Formation (fig. 4), which consists of a clastic redbed sequence of brown to variegated siltstone, waxy red shale, calcareous sandstone, and some gray to reddish buff limestone and conglomerate (Wengert and Matheny 1958). The Molas represents the first sediments deposited in the subsiding Para-

\*A thesis presented to the Department of Geology, Brigham Young University, in partial fulfillment of the requirements for the degree Master of Science, August 1977; James L. Baer, thesis chairman.

TABLE 1  
LOGS AND DRILLING DATA PROVIDED BY THE AMERADA PETROLEUM CORPORATION

Well No.	Location (section)	Cored Interval (in meters)	Thickness Cored (meters)	Type of Log
1	17	+1245-+1222	23	Gamma
2	17	+1239-+1209	30	Gamma, Neutron
3	17	+1259-+1238	21	Gamma, Resistivity
4	17	+1271-+1248	23	Gamma, Resistivity
5	20	+1299-+1275	24	Gamma, Resistivity Self-Potential
6	26	+1259-+1216	43	Gamma
7	25	+1196-+1166	30	Gamma, Neutron
8	31	+1363-+1267	96	Gamma
9	5	+1249-+1226	23	Gamma, Neutron

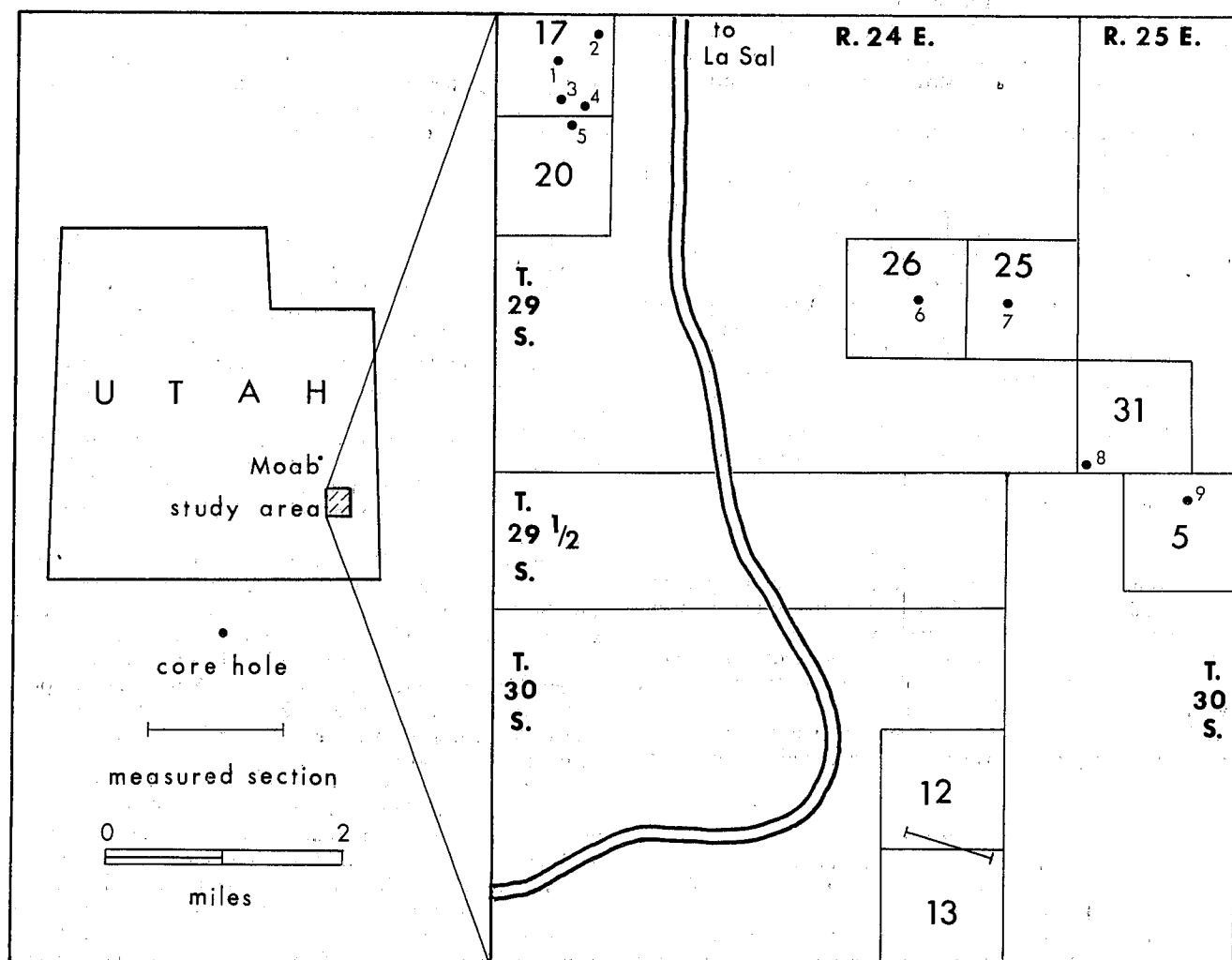


FIGURE 1.—Index map showing study area and location of cores.

dox Basin. Overlying the Molas Formation is the Pinkerton Trail Formation (fig. 4), which is composed of fossiliferous limestone and dolomite interbedded and underlain by dark to light-gray silty shale (Clair 1958) and shows a continuation of the tectonic style observed in the Molas Formation. Overlying the Pinkerton Trail Formation is the Paradox Formation (fig. 4), a cyclic deposit consisting of several members. The lower member is composed of anhydrite, dark-gray shale, gray dolomite, and cherty limestone. The middle member is composed of interbedded salt, black shale, black calcareous siltstone, gypsum, anhydrite, and dolomite in the middle of the basin, which grades shelfward into biohermal-biostromal dolomitic limestone (Wengerd and Matheny 1958, Clair 1958). Toward the Uncompahgre, the Paradox Formation grades into or intertongues with an arkosic sandstone, composed of eroded material from the uplift. The Paradox Formation shows deposition in a restricted basin with a stable shelf to the south and west, and a fault-bounded block (Uncompahgre) uplifted on the northeast. The salt deposits of the middle member of the Paradox Formation form salt anticlines and have a local effect on deposition from Pennsylvanian through Triassic time. The Lisbon Valley fault and anticline are the result of this salt movement (Kelley 1955). The upper member of the Paradox Formation is much like the lower member and represents a change to a basin with a normal marine environment (Wengerd and Matheny 1958). Overlying the Paradox Formation is the Honaker Trail Formation which is composed of biohermal dolomites (fig. 4).

Northeast near the Uncompahgre, the Honaker Trail Formation is composed dominantly of coarse micaceous and arkosic sandstone. The Honaker Trail Formation represents the beginning of rapid uplift of the Uncompahgre and the change in basin deposition from shales, evaporites, dolomites, and limestones to coarse arkosic sandstones. The Permian is characterized by a change from marine-clastic deposition to sub-aerial clastic deposition. The Cutler Formation in the Paradox Basin consists of more than 2400 m of coarse arkose and conglomerate adjacent to the Uncompahgre uplifted block. The formation thins southeast to 520 m of arkosic sandstone intertongued with shale and some limestone. The Cutler Formation represents a time of rapid uplift of the Uncompahgre, shedding a volume of sediment great enough to fill the sinking Paradox Basin. The Triassic system in the Paradox Basin is represented by the Moenkopi and Chinle formations and part of the Glen Canyon Group. The Moenkopi Formation, which unconformably overlies the Cutler Formation, consists of red shales, siltstones, and sandstones (Robeck 1958). The Moenkopi Formation is not found in Lisbon Valley. Units of the Chinle Formation unconformably overlie Permian rock in the Lisbon Valley area (Weir and Puffett 1958). The Chinle Formation has been divided into Temple Mountain Member, siltstone, mudstone, and conglomerate; Shinarump Member, sandstone and conglomerate; Monitor Butte Member, predominantly mudstone, claystone, sandstone; Moss Back Member, mudstone, siltstone, sandstone, and conglomerate; Petrified Forest Member, claystone, mudstone, siltstone, and

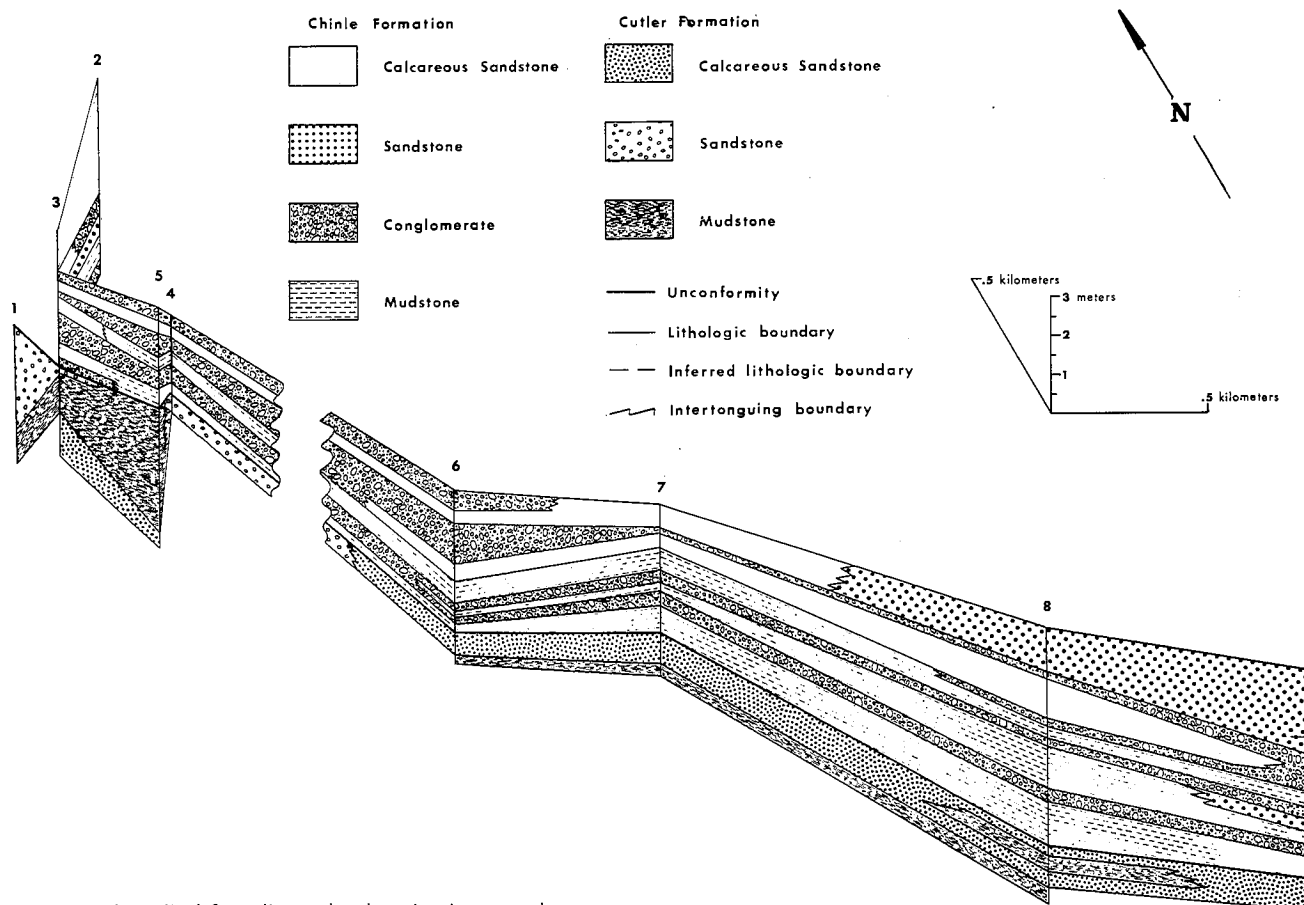


FIGURE 2.—Generalized fence diagram based on the nine cores taken.

TABLE 2  
CORE COMPOSITION

Formation	Core No.	Depth of Sample in Meters	Mineral Composition Percent					Matrix %	Cement %	Rock Type
			Quartz	Feldspar		Mica				
				Potassium	Plagioclase	Muscovite	Biotite			
Chinle	6	841.33	49	30	6	2	10	36		arkosic wacke
Chinle	4	759.92	64	22	2	8	2	36		arkosic wacke
Chinle	6	852.16	54	32	2	6	6		30	calcareous arkose
Chinle	6	835.47	58	28	2	4	8	25		arkosic wacke
Chinle	9	783.41	52	32	0	10	6		30	calcareous arkose
Chinle	8	769.61	50	28	2	8	12		20	calcareous arkose
Chinle	7	847.31	49	27	4	8	12	70		sandy mudstone
Chinle	2	787.30	50	36	8	2	4		29	conglomerate
Chinle	5	746.86	52	34	6	5	3		34	conglomerate
Cutler	8	822.95	58	22	0	8	12		41	calcareous arkose
Cutler	1	796.65	54	30	0	8	8		32	calcareous arkose
Cutler	3	805.85	56	32	4	6	2	30		arkosic wacke
Cutler	1	791.15	60	30	0	10	0	38		arkosic wacke
Cutler	3	804.19	58	29	3	8	2			sandy limestone

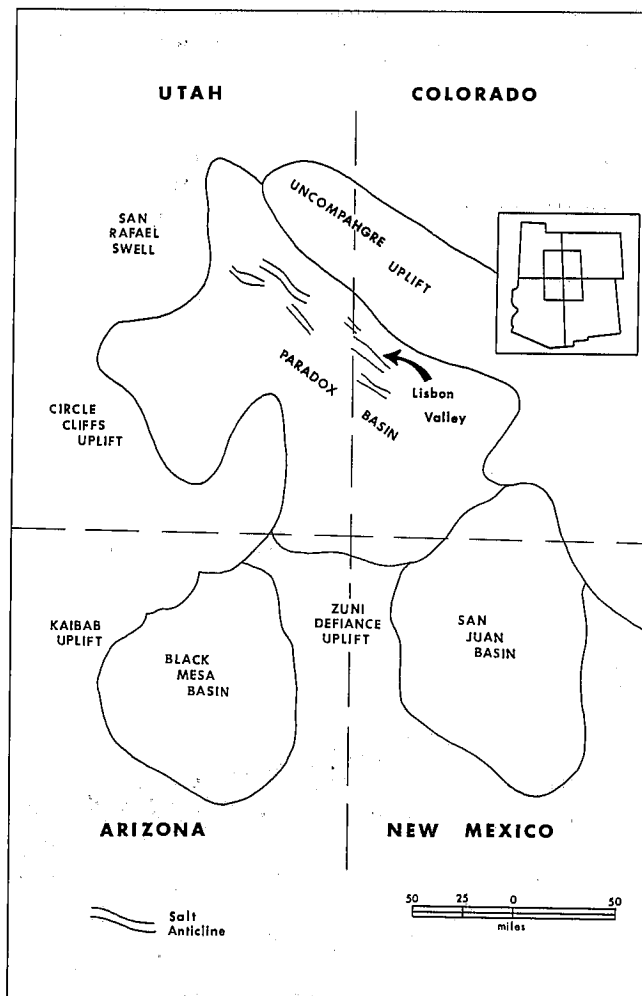


FIGURE 3.—Map of Lisbon Valley showing relative positions of surrounding formations.

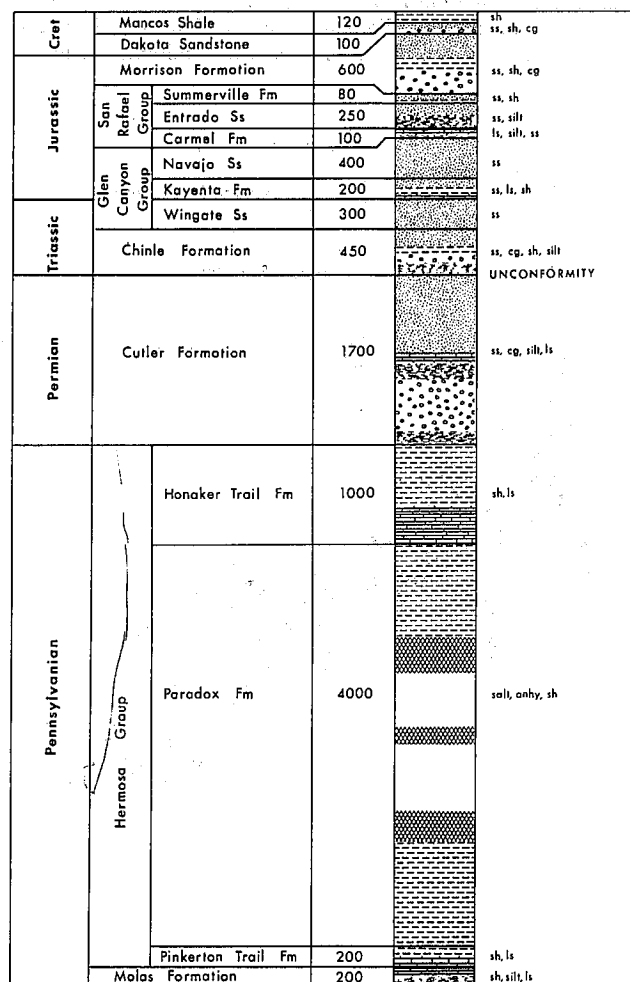


FIGURE 4.—Stratigraphic column.

sandstone; Owl Rock Member, predominantly siltstone and limestone; and Church Rock Member, siltstone and sandstone. In Lisbon Valley the Moss Back Member overlies the Permian Cutler Formation (Stewart et al. 1972).

The Glen Canyon Group makes up the Triassic and Lower Jurassic rocks that crop out in Lisbon Valley (fig. 4). Formations in the Glen Canyon Group are the Wingate Sandstone, a dominantly windblown sandstone unit, the clastic and carbonate facies of the Kayenta Formation, and the Navajo Sandstone. The San Rafael Group of Jurassic age in Lisbon Valley consists of the Carmel Formation, Entrada Sandstone, and Summerville Formation. The Morrison Formation, consisting of the Salt Wash Member and the Brush Basin Member, was the last Jurassic formation deposited in the Lisbon Valley area.

Cretaceous deposits, Dakota Sandstone and Mancos Shale (Wright and Dickey 1958), are the youngest consolidated units found in the Lisbon Valley area.

#### Structure

Lisbon Valley lies in the Paradox fold-and-fault belt, a tectonic region dominated by northwest-trending folds and faults (Kelley 1955). Fold structures in Lisbon Valley are the Lisbon Valley anticline and the Disappointment syncline. The anticline's southwest flank dips 8°, and the northwest flank dips 6° into the Disappointment syncline (Lekas and Dahl 1956, Weir and Puffert 1958). The Lisbon Valley fault, one of the major faults in the Paradox fold-and-fault belt, faults the Lisbon Valley anticline and has a maximum displacement of 1220 m which decreases toward the nose of the anticline. The fault dips approximately 60° northeast and is broken along a single surface in the central part of the structure but branches and becomes a fault zone at the nose of the anticline (Lekas and Dahl 1956).

Lisbon Valley has been affected greatly by salt movement. Both fold structures and faulting are the direct result of movement.

#### CUTLER STRATIGRAPHY

The Cutler Formation is the oldest penetrated by the cores used in this study. Penetration into it ranged from 3 m to 26 m. The upper 7.5 m of the Cutler Formation were measured in outcrop. Rock types found in the cores were sandstone and mudstone with minor lenses of limestone. The outcrop section consisted of sandstone and shale. No fossils were found in the samples examined.

#### Sandstones

Two lithologically distinct sandstone types made up the major part of the Cutler Formation that I observed. In accordance with the classification of Pettijohn (1975), the two types of sandstones are calcareous arkose and arkosic wacke.

##### *Calcareous arkose* (fig. 5)

Color ranges from medium to dark red-brown, with some white patches and dark gray bands. Grains range in size from 0.5 mm to 0.1 mm with the most abundant grain size being 0.125 mm. Subangular grains dominate. Cutler Formation arkoses have a typical mineral composition of 54-58 percent quartz, 22-30 percent potassium feldspar, traces of plagioclase feldspar, and 16-20 percent muscovite and biotite (table 2). Mica flakes show a preferred orientation with their basal surfaces parallel to the bedding. The dark red-brown and dark gray bands which are unevenly spaced through the cores are

composed of micaceous mudstone and range in thickness from 1 mm-2 cm. The cores tend to break along these dark bands, usually exposing a surface with abundant mica flakes. The attitude of these bands varies from horizontal to about 30° and is the only bedding observed in the cores. Only horizontal bedding was observed in the outcrop section; however, a small channel deposit about 1 m thick and 6 m across was observed a short distance laterally from the outcrop section.

Calcareous arkose samples are cemented by sparry calcite and dolomite, which range from 32-40 percent of the bulk composition of the samples for which an analysis was done. Dolomite rhombs are found in bands 1-2 cm thick in a sparry calcite cement in about one-third of the samples examined. These bands appear to be the result of secondary dolomitization of the dark-colored mudstone bands. The red coloring dominant in most samples is the result of red stain in the cement, probably from ferric oxide. Stain is darkest at the contact between grains and cement. White areas do not differ from red areas in composition but could have resulted from leaching by H<sub>2</sub>S and carbonate waters (Keller 1953).

##### *Arkosic wacke* (fig. 6)

Color ranges from light to dark red-brown with white patches, and dark red-brown and dark gray bands. Subangular grains, which compose 30-38 percent of the bulk composition

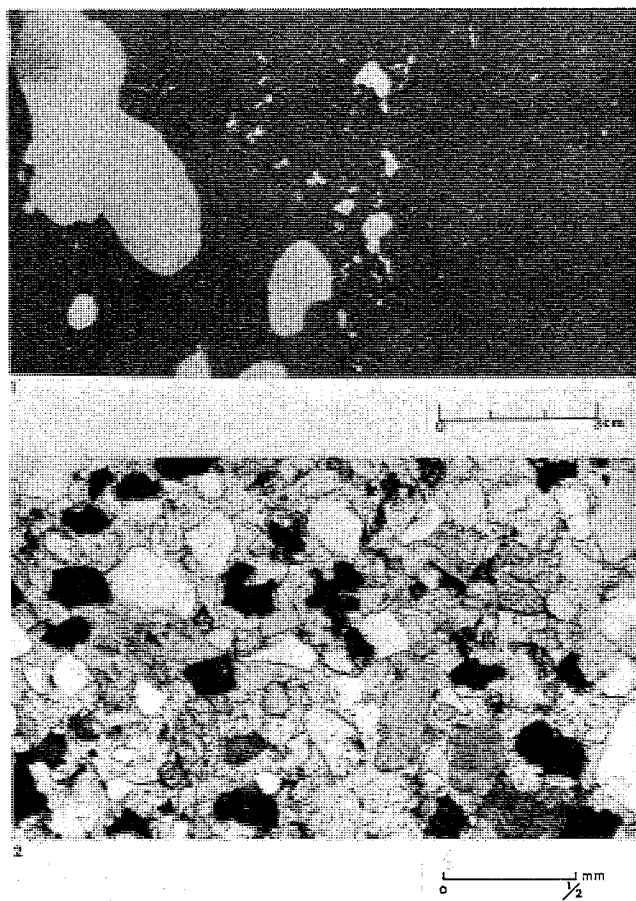


FIGURE 5.—Cutler Formation calcareous arkose, medium grained; mottled, white, lavender, and red; grains are quartz, feldspar, and mica; thin mudstone lenses; sparry calcite cement. Photo 1.—Depth 807.25 m in well 3. Photo 2.—Depth 852.16 m in well 6.

of the samples for which detailed analysis was done (table 2), are composed of 56-60 percent quartz, 30-32 percent potassium feldspar, 0-4 percent plagioclase feldspar, and 8-10 percent muscovite and biotite. As in the calcareous arkoses, micas are abundant in the dark bands, which also contain mudstone, calcite, and dolomite. Dark bands appear to be more numerous in the arkosic wacke units than in the calcareous arkose units.

Percent of matrix ranges from 30 to 40, dominantly silt and clay with the dominant matrix materials, calcite and dolomite in varying quantities through the units, but never more than 15 percent of the matrix. The red-brown stain found in the arkosic wacke units is evenly spread through the mudstone matrix, except for the leached areas, and is the result of the same process as that in the calcareous arkose units.

Cross-bed sets, commonly 5 cm thick or less, are found in about half the samples. The only other bedding found is that shown by the dark bands.

#### Mudstones

Mudstone makes up less than 40 percent of the total Cutler Formation section in the cores examined. However, locally, mudstone may dominate, as in core 5 (fig. 2). Two

different mudstone lithologies were observed in the cores examined (fig. 7).

#### Sandy Mudstone

The sandy mudstone is dark red-brown with white patches and gray-green bands. The dominant mineral grains are subangular 0.2 mm to 0.02 mm quartz, potassium feldspar, plagioclase feldspar, muscovite, and biotite. Sparry calcite stringers, as well as thin bands of calcite and dolomite rhombs, are found as minor components of the sandy mudstone units. Calcite and dolomite compose less than 10 percent of the sandy mudstone units.

Parting is shown in thin bands containing abundant mica. Cross-bedding is found in about half the samples examined. Rounded and flattened clasts of mudstone are found within several mudstone units and probably represent rip-up clasts. The red coloring of the mudstone unit is interpreted as the result of the processes that formed the color in the sandstone units.

#### Mudstone

The mudstone units are dark red-brown with white patches and very dark red-brown and dark gray-green bands. The micas tend to be concentrated in the dark bands and show parting. Small scale cross-bedding, 10 cm and less, is

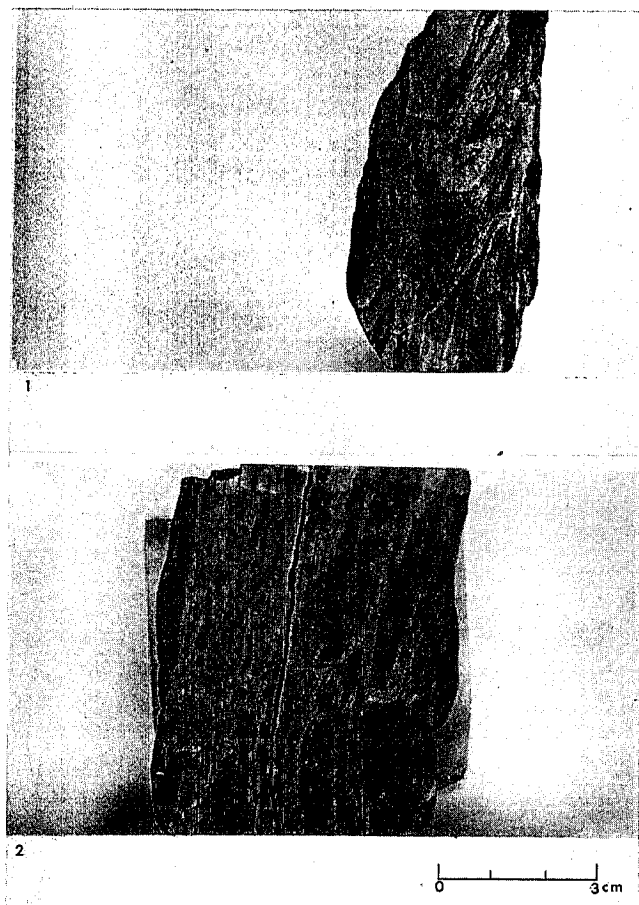


FIGURE 6.—Cutler Formation arkosic wacke, fine grained; dark red with lighter red and white bands; mudstone matrix. Photo 1.—Depth 806.15 m in well 3. Photo 2.—Depth 796.65 in well 1.

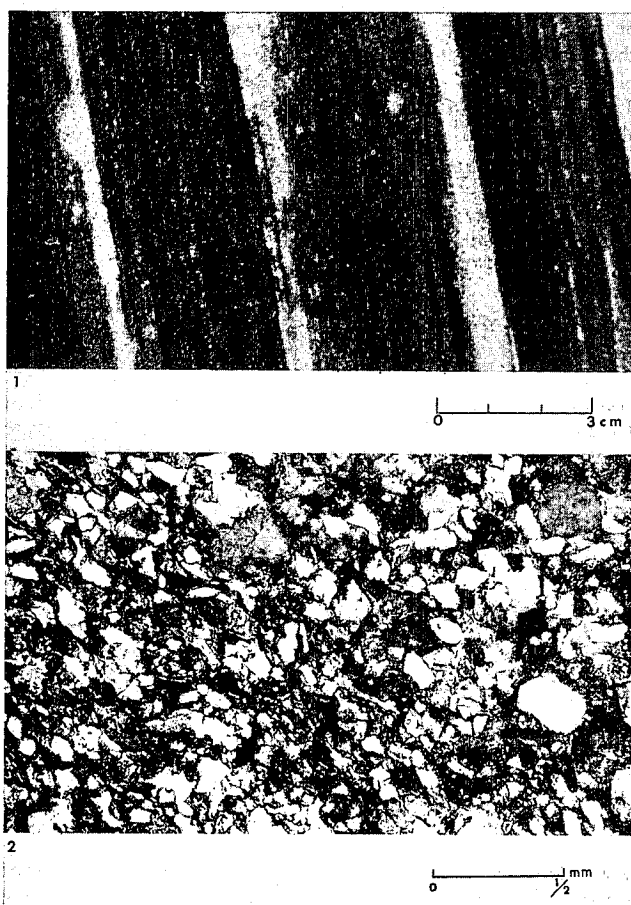


FIGURE 7.—Photo 1.—Chinle Formation sandy mudstone, dark red-brown with light gray bands; convolute bedding. Depth 789.26 in well 3. Photo 2.—Cutler Formation calcareous mudstone, dark red with light gray patches. Depth 804.44 in well 3.

found in about half the samples examined. Calcite is found as sparry stringers and crystalline cement.

A continuous sequence from mudstone to sandy mudstone to arkosic wacke exists in the cores examined, reflecting possible changes in the energy of deposition.

#### Sandy Limestone

One limestone unit 50 cm thick, composed of 70 percent calcite and dolomite, was found in well 3. The unit is sandy and sparry. Detrital mineral grains were subrounded 0.12 mm and less, consisting of 58 percent quartz, 29 percent potassium feldspar, 3 percent plagioclase feldspar, 8 percent muscovite and 2 percent biotite. The limestone unit appears to be the result of alteration of a sandy mudstone unit (fig. 8).

#### CHINLE STRATIGRAPHY

The Moss Back Member of the Chinle Formation overlies the Cutler Formation with no detectable angular discordance in the study area. Three major lithologic types were observed in the Moss Back Member; sandstone, mudstone, and conglomerate. The cored interval of the Moss Back Member used in this study is shown in figure 9. No identifiable fossils were found in the sandstone and mudstone units studied.

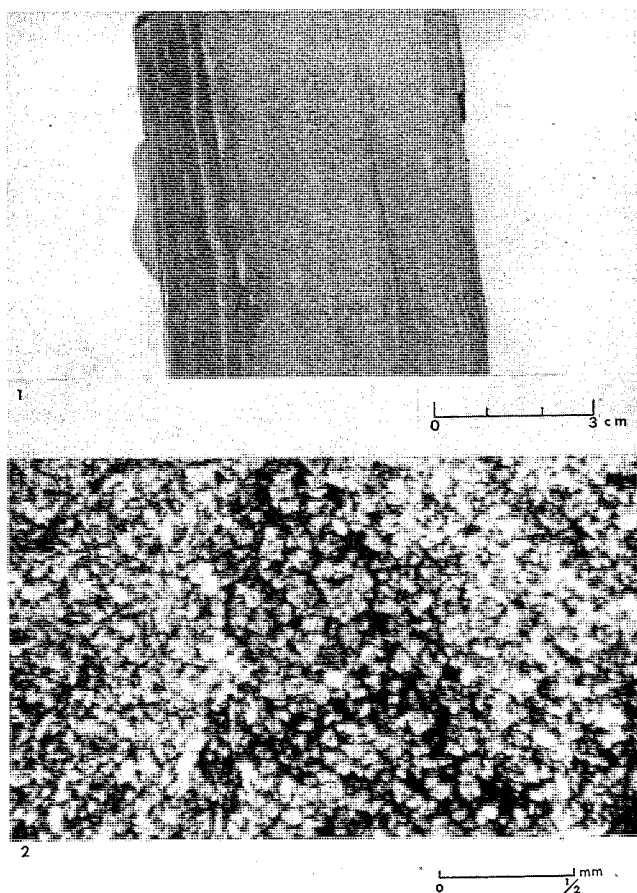


FIGURE 8.—Cutler Formation sandy limestone; quartz feldspar and mica grains; dolomite rhombs; calcite cement; dolomite rhombs are poorly preserved and occur in bands. Photos 1 and 2.—Depth 772.89 in well 4.

One sample of conglomerate which contained fossils will be discussed in the section on conglomerates.

#### Sandstone

Sandstone is the dominant lithology in about half the cores examined (fig. 2). Two lithologically distinct sandstone types were observed. These are calcareous arkose and arkosic wacke (Pettijohn 1975).

#### Calcareous arkose (fig. 10)

Color in the calcareous arkose units is light to medium gray with dark gray-green bands. Mineral grains range in size from 0.06 mm to 0.5 mm, with 0.1 mm to 0.25 mm size dominating. Grains are angular to subangular, becoming rounded as grain size increases. Mineral composition of the units consists of 50-54 percent quartz, 28-32 percent potassium feldspar, 0-2 percent plagioclase feldspar, and 12-20 percent muscovite and biotite (table 2). Mica content is highest in the dark bands which also have abundant mudstone as matrix material. Carbonaceous material, occurring in thin plates to 2-cm bands, and pyrite are found in most samples. Pyrite is never found except in association with carbonaceous material in the samples examined.

Horizontal bedding and cross-bedding, with cross-bed sets 20 cm and smaller, are the two most common bedding types found. Also a common occurrence is bedding that appears to dip at an angle of 30°. This could be the result of large-scale cross-bedding. Graded bedding and convolute bedding are common, and load structures and ripple marks were found in a few samples. Climbing ripples were found in one sample.

The calcareous arkose units are cemented by sparry calcite and dolomite, which ranges from 20-30 percent of the bulk composition of the units. The cement completely surrounds grains in the coarser units, but not in most of the finer-grained ones.

#### Arkosic wacke (fig. 11)

Arkosic wacke units are light gray with dark gray-green bands. Grains range from 0.06 to 0.2 mm in diameter and are composed of 49-60 percent quartz, 22-30 percent potassium feldspar, 2-6 percent plagioclase feldspar, and 10-12 percent muscovite and biotite (table 2). Micaceous material and pyrite are present in most samples. Carbonaceous material is found as black slivers to 5-mm-thick bands.

Cross-bedding, with sets 5 cm and less, and horizontal bedding are again dominant bedding types. Also abundant are beds dipping at about 30° which probably represent large-scale cross-bedding. Also found in some samples are ripple marks, load structures, and convolute bedding.

Grains are surrounded by a silt and clay matrix with microcrystalline calcite and dolomite. The matrix comprises 25-30 percent of the bulk composition of the arkosic wacke units. Calcite and dolomite make up less than 10 percent of the matrix. Some sparry calcite and dolomite are found in fractures, mainly in the carbonaceous material.

#### Mudstone

Two types of mudstone were found in the cores examined. These are sandy mudstone and mudstone. A continuous sequence of rock types exists from sandstone to sandy mudstone to arkosic wacke (fig. 7).

#### Sandy Mudstone

Color in the sandy mudstone units is dark gray to green-gray, with minor dark red-brown in some samples. Mineral

grains consist of 0.1 mm to 0.06 mm subangular quartz, 49 percent; potassium feldspar, 27 percent; plagioclase feldspar, 4 percent; muscovite and biotite, 20 percent. Also found in some sandy mudstone samples are mudstone intraclasts which are well rounded and, in some cases, flattened. Carbonaceous material with occasional pyrite is found, but only in minor amounts. Convolute bedding is the main type found. Less common sedimentary structures are slump structures, ripple marks, cross-bedding, and horizontal bedding. When samples were washed, they broke into fragments that resembled "pencil shale."

Microcrystalline calcite and dolomite are found in small quantities in some samples. Some stringers of sparry calcite and dolomite were found.

#### Mudstone

Mudstone units are gray to dark gray-green with some samples showing a dark red-brown color. Samples examined contain muscovite and biotite flakes and mudstone intraclasts that are well rounded and flattened. Minor amounts of carbonaceous material and pyrite were also found disseminated throughout the samples with some sparry stringers.

The major sedimentary structure found is convolute bedding. Less numerous types found include ripple marks, cross-bedding, and slump structures. After washing, some samples broke into fragments resembling "pencil shale."

#### Conglomerate

Two types of conglomerate were distinguished; however, the mineral composition is very similar (table 2) and characteristics are similar. The only observable difference is in the

shape of the mudstone clasts, i.e., rounded or flattened. Therefore, the descriptions given below will include both.

#### Mudstone Conglomerate (fig. 12)

Color in the mudstone conglomerate varies with clast type from light to medium gray. Clasts range in size from 7 cm to 2 mm, with an average size ranging from 2 to 4 cm. Clasts are generally well rounded, but some angular ones are found. Both flattened and spherical clasts are found and can occur in the same sample. Flattened clasts dominate slightly over spherical ones. Clasts are composed of mudstone with lesser amounts of claystone, sandstone, and limestone. Mudstone and claystone clasts are the only ones that occur flattened. Two types of mudstone clasts are found. The most abundant type is light gray with abundant 0.1 mm to 0.06 mm grains. These mudstone clasts appear to have the same composition as the sandy mudstone units previously described. The second type of mudstone clast appears to be of the same composition as the previously described mudstone units.

Mineral grains are found between the clasts in all but a few of the samples examined. Grains are subangular to rounded, the degree of roundness increasing with grain size, and range from 0.06 mm to 1 mm. Mineral types are quartz, 50-52 percent; potassium feldspar, 34-36 percent; plagioclase feldspar, 6-8 percent; muscovite and biotite, 6-8 percent. Carbonaceous material is found in beds as thick as 2 cm but is commonly found as thin plates and slivers.

Bedding types found consist of cross-bedding, graded bedding, and convolute bedding.

Cement in all samples is sparry calcite and dolomite, which composes from 30-40 percent of the bulk composition

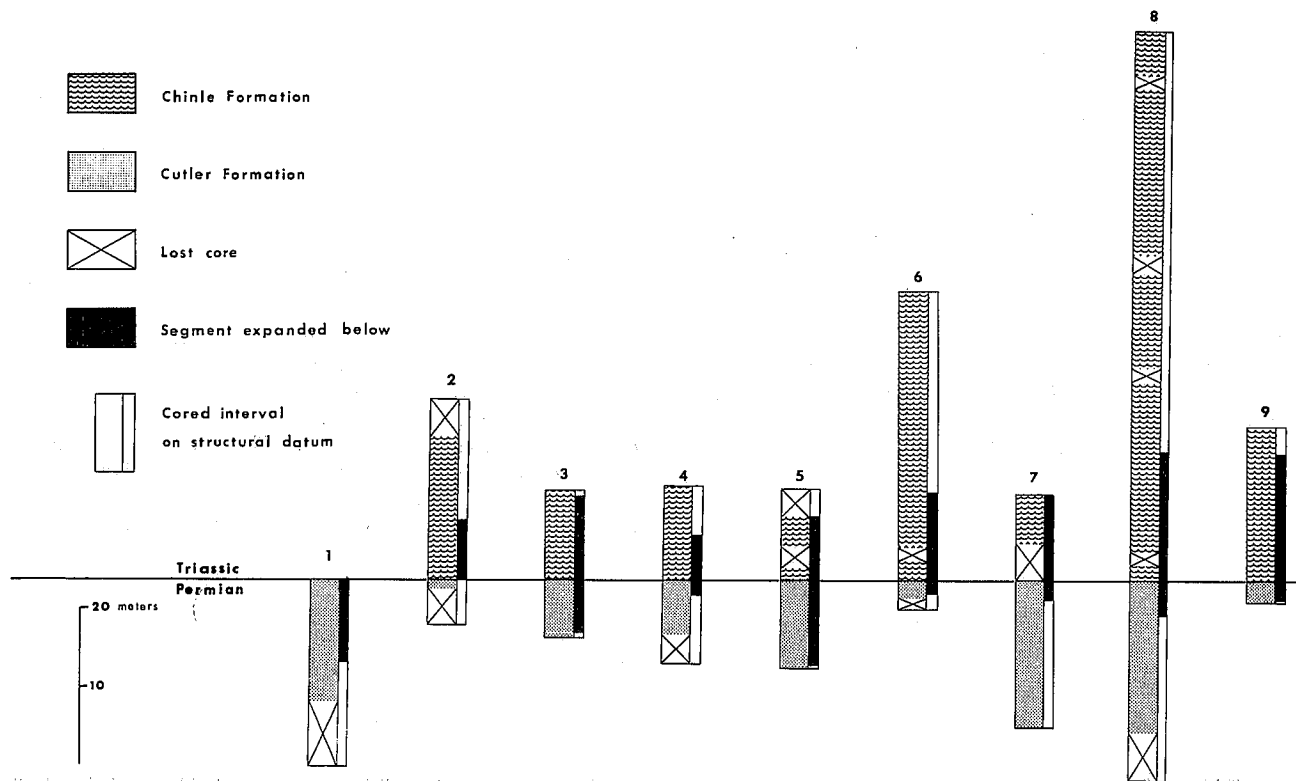


FIGURE 9.—Diagram of cores, showing the Moss Back Member of the Chinle Formation and the Cutler Formation.



of all samples studied except in core 9. Individual calcite and dolomite grains range in size from 1 mm to 0.05 mm. Core 9 (fig. 2) has the smallest cement grains and was the only core that had an abundant silt and clay matrix, ranging from 10-20 percent. This core also contained more dolomite as cement than the other cores. Sparry calcite and dolomite are also found in fractures in the carbonaceous material and in the center of many mudstone clasts.

Fossils found are leaf imprints in the carbonaceous material and gastropods. The leaf imprints were not identifiable. The gastropods are in mudstone clasts that have undergone transport and cannot be positively linked with the formation under study.

Interbedded conglomerate and sandstone are found in some cores. These occur in thin, less than 15-cm, beds of alternating conglomerate and sandstone. The lithologies are as described under calcareous sandstone and mudstone conglomerate. These units are an example of graded bedding.

Outcrop units described as the measured section (appendix) follow the lithologic descriptions given for the subsurface units.

#### STRATIGRAPHIC CORRELATION

Correlation of strata between cores 1-5 and 6-9 is good

(fig. 2). However, between cores 4 and 6, a gap of 6000 m exists where no data is available. Therefore, the correlations shown in figure 2 and discussed below are somewhat uncertain between cores 4 and 6. Correlation of the surface and subsurface data was not attempted in figure 2 because of the distance involved and the lack of good exposures at the outcrop. However, general comparison will be used between surface and subsurface data in the following discussion.

In cores 1-5, core 3 was chosen as the one from which correlations to the other four will be made. A detailed description of the lithology found in core 3 is given in the appendix. Although no thin sections were obtained across the unconformity in cores 2-5, a study of the strata directly overlying and underlying it indicates it is a distinct boundary. The unconformity is recognized in both outcrop and core by the change in color from the light grays found in the Moss Back Member of the Chinle Formation to the red-brown of the Cutler Formation. Also distinctive in the cores and outcrop studied is the lack of conglomerate and carbonaceous matter in the Cutler Formation. The Moss Back Member of the Chinle Formation and the Cutler Formation in the study area have very similar types of sedimentary structures and mineral compositions (table 2). In each case in cores 2-5, the core broke at the place where the unconformity was in-

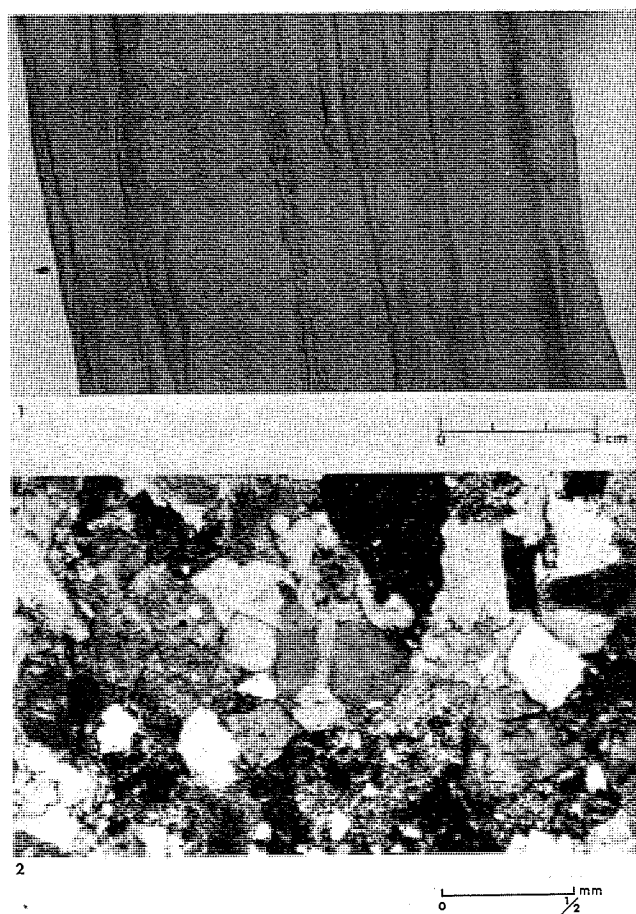


FIGURE 10.—Chinle Formation calcareous arkose, fine to medium grained; light gray with some darker bands, cross-bedding, and ripple marks. Photo 1.—Depth 788.38 m in well 3. Photo 2.—Depth 759.92 in well 4.

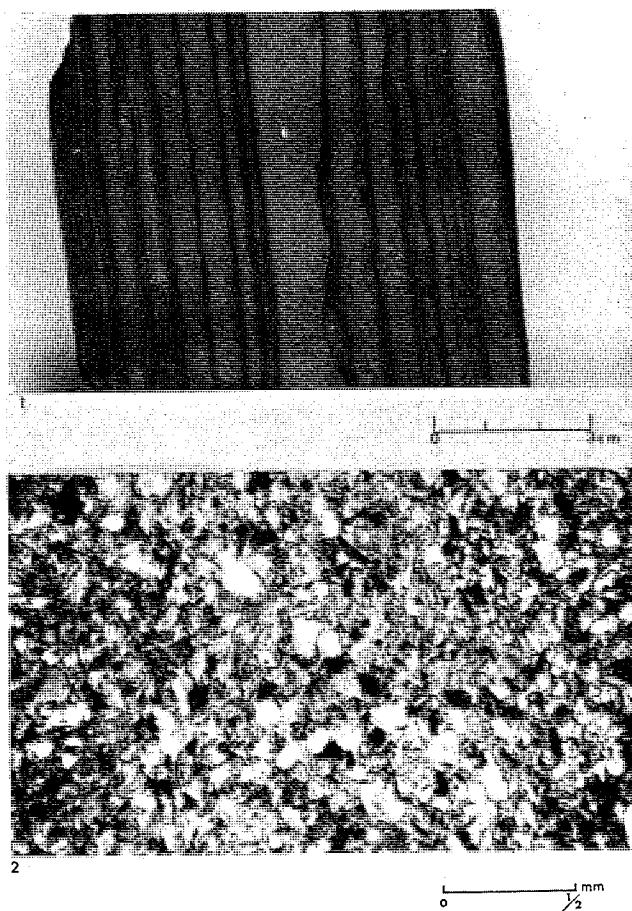


FIGURE 11.—Chinle Formation arkosic wacke, fine grained; light gray with dark bands; ripple marks. Photo 1.—Depth 790.65 m in well 3. Photo 2.—Depth 822.95 in well 8.

licated. However, upon examination of the broken ends of the core, no weathered surface or paleosoil could be found. Underlying the unconformity in wells 2, 3, and 4 is a calcareous arkose that varies in thickness from 20-63 cm. In well 1, the Cutler Formation underlying the unconformity is composed of 811 cm of arkosic wacke. In core 5 a sandy mudstone unit 944 cm thick underlies the unconformity. At the outcrop section the Cutler Formation directly underlying the unconformity is mostly sandstone; however, in one place a mudstone unit that appears to be the result of filling of a small channel, about 6 m wide and 1 m deep was found. However, this mudstone unit cannot be definitely placed in the Cutler Formation and might represent the erosion and filling of channels by the stream that deposited the Moss Back Member of the Chinle Formation. Overlying the Permian-Triassic unconformity in wells 2 through 5 are calcareous arkosics of the Moss Back Member of the Chinle Formation, that range in thickness from 7 cm to 140 cm. Although similar in composition (table 2) to arkose units in the Cutler Formation, the calcareous arkoses overlying the unconformity do not appear to be the result of erosion of the Cutler Formation.

The stratigraphic sequence found in cores 1-5 is shown on the generalized fence diagram in figure 2. The Cutler For-

mation studied in cores 1-5 changes from a mudstone-dominated facies in cores 3 and 5 to one dominated by calcareous arkose in cores 1, 2, and 4. A lens of sandy limestone occurs in core 3 that cannot be correlated to any other of the surrounding cores. As stated in the previous section on stratigraphy, the sandy limestone units appear to be the result of secondary calcite and dolomite infilling. Other cores have units with a high percentage of calcite and dolomite cement, but it does not exceed 41 percent of the total composition of the rock. The Moss Back Member of the Chinle Formation as seen in cores 4 and 5 is dominated by three conglomerate units with minor calcareous arkose and mudstone units. In core 3 the upper conglomerate unit has pinched out, and in its place are found two thin mudstone units that thicken northward to core 2, a calcareous arkose unit that continues to core 2, and an arkosic wacke unit that pinches out between cores 3 and 2. The two lower conglomerate units are found in cores 2-5, but thin from a maximum of 274 cm and 184 cm in core 5 to 80 cm and 74 cm in core 2. Conglomerate units grade upward into sandstone units that in most cases overlie the conglomerate. In core 4 the lower conglomerate unit has several interbedded calcareous arkose lenses that exhibit graded bedding. Above the Permian-Triassic unconformity about 7 cm in core 3 is found a conglomerate

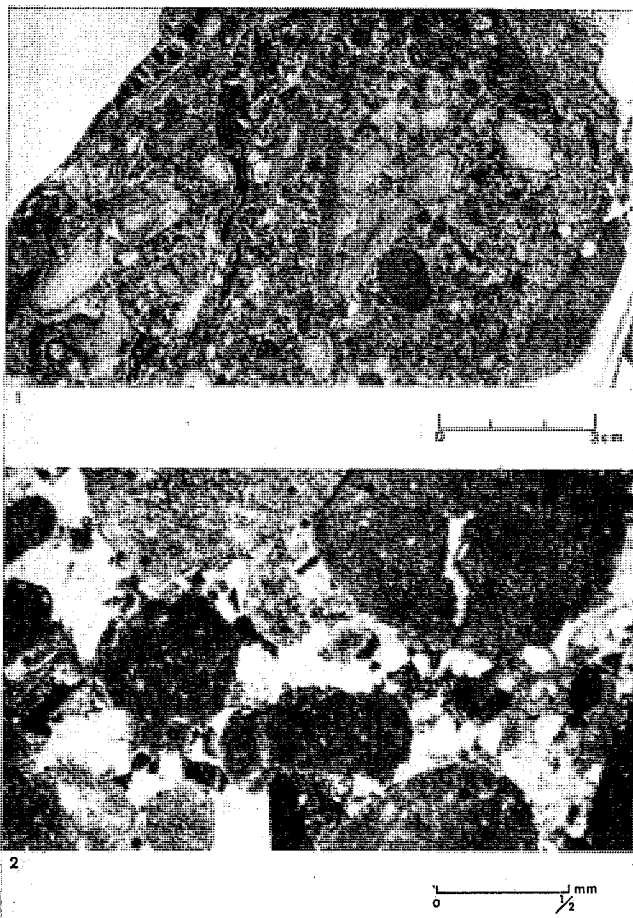


FIGURE 12.—Chinle Formation conglomerate; clasts 4 cm and smaller, mudstone; black areas are organic matter with calcite fracture filling; calcite cement. Photo 1.—Depth 745.68 m in well 5. Photo 2.—Depth 766.51 in well 4.

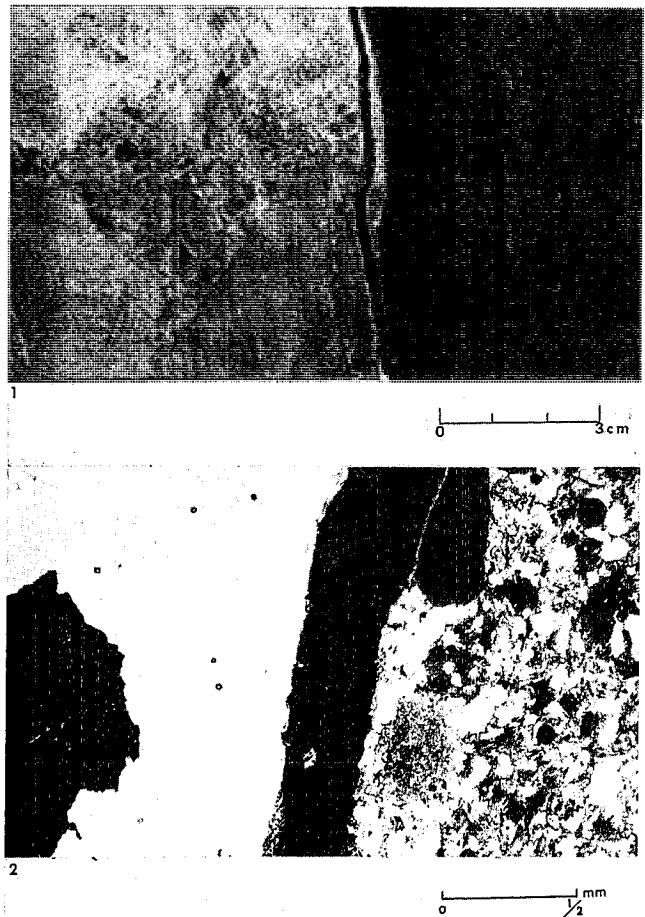


FIGURE 13.—Cutler and Chinle formations. Unconformity is in center of both top and bottom photographs. Depth 822.85 in well 8.

lens that appears to grade laterally into mudstone in cores 5 and 2. The change in the overall character of the cores from coarser grained in cores 4 and 5 to finer grained in core 2, with core 3 being about halfway through the transition, indicates a decrease in the energy of the depositional medium.

In cores 6 through 9, correlations appear to be good, although the distance between cores is greater than between 1 and 5. A description of core 9 is given in the appendix. Core 9 is used because it is complete. The Permian-Triassic unconformity is shown in figure 13. Core 8 was the only core in which the section of the core containing the unconformity was found intact. Examination of the section of the core containing the unconformity before it was cut revealed a sharp contact with no indication of weathering and no paleosol development. The contact appeared to have a thin (less than 0.5 mm) stringer of calcite between the two formations. When the section of the core containing the unconformity was cut, the core broke and was put back together with epoxy. The epoxy holding the pieces of the core together is the black band running across the photomicrograph in figure 13. The only indication that possible weathering action took place along the unconformity is the 1- to 2-cm band of red-brown color that appears to be lighter than the color immediately below it. Cores 6 and 9 broke along the unconformity before I examined them. From examination, however, I conclude that they are similar to core 8. The core from the interval directly above the unconformity in core 7 was not recovered. The Cutler Formation in cores 6 through 9 consists of a calcareous arkose unit directly underlying the unconformity which is underlain by a mudstone unit. Core 8, which penetrated 28.01 m, of which 12.66 m were recovered, of the Cutler Formation consists of alternating arkose, arkosic wacke, mudstone, and sandy mudstone. Cores 6, 7, and 9 did not penetrate the Cutler formation as far as core 8. Therefore, no extensive comparison can be made.

Correlation of the Moss Back Member of the Chinle Formation in cores 6-9 is made difficult by the 488 cm of core missing above the unconformity in core 7. The missing part of core 7 probably consists of a thin conglomerate unit directly overlying the unconformity as is found in cores 6 and 8. Core 9 has a 29.2-cm calcareous arkose unit directly overlying the unconformity. Core 9 has six conglomerate units ranging from about 6 cm to 149 cm thick that appear to be correlative with conglomerate units in cores 6, 7, and 8. Conglomerate units are thickest in cores 6 and 9, and thin to cores 7 and 8. Core 6 has several conglomerate units that appear to interfinger with calcareous arkose units in core 7. Core 9 contains several arkosic wacke units that are correlative with arkosic wacke units in core 8 and appear to interfinger with calcareous arkose units in core 7. Two other arkosic wacke units found in the lower part of core 9 appear to interfinger with mudstone units found in core 8. The upper part of core 7 is dominated by calcareous arkose units in core 6. A mudstone facies dominates the lower parts of cores 7 and 8 but thins in core 6, where conglomerate appears to replace it, and 9, where it interfingers with arkosic wacke units.

In several parts of cores 6-9 conglomerates and arkosic wacke or calcareous arkose units are interbedded. The units typically are 6 to 20 cm thick and show graded bedding from conglomerate to sandstone. Also abundant in interbedded units are ripple marks and cross-bedding.

The depositional environment of cores 6-9 appears to have decreased in energy from cores 6 and 9 toward cores 7 and 8; at least in the lower part of the cores. The upper

parts of cores 6-9 appear to show an increase in energy of the depositional environment.

The large distance between cores 4 and 6, as shown in figure 2, is dominated by conglomerate facies. The conglomerate units appear to thicken and coalesce in core 4 while thinning and interfingering with sandstone units in core 6. However, because the distance between cores 4 and 6 is greater than the distance between cores 1-4 or cores 6-9, the correlations given are not as reliable as the other correlations.

An overall analysis of the cores studied suggests that relatively thin, but laterally extensive units of conglomerate and mudstone extend throughout the study area, while arkosic wacke and (to a lesser extent) calcareous arkose units occur as lenses in the Moss Back Member of the Chinle Formation. The Cutler Formation, in the cores examined, appears to consist of relatively thick and laterally extensive sandstone and mudstone units. Analysis of the mineral content of the Moss Back Member of the Chinle Formation and the Cutler Formation in the cores studied indicates that they do not differ significantly. However, as was stated in the discussion of the Permian-Triassic unconformity and the strata directly overlying it, the Moss Back Member of the Chinle Formation does not appear to consist of components that were eroded from the Cutler Formation. The similarity between the mineral components of the Cutler Formation and of the Moss Back Member of the Chinle does indicate that the source of the two units was the same.

The nature of the Permian-Triassic unconformity in the study area is indicated by the lack of any signs of erosion or paleosol development and the sharpness of the boundary. The features just stated indicate that the study area was one of nondeposition during the Lower Triassic. Whether this area of nondeposition was subaerial or subaqueous is not clear. Because no soil or erosional surface developed along the unconformity, it would appear that the area was submerged. This supposition, however, may be inconsistent with the fluvial depositional environment ascribed to the Cutler Formation, at least in the upper part, and to the Moss Back Member of the Chinle Formation.

## APPENDIX

### Measured Section

Sections 12 and 13, T. 30 S, R. 24 E, 100 m south of Mivida mine and 50 m north of an unnamed mine entrance, San Juan County, Utah. Beds strike 10 NE and dip 11°.

Unit	Description	Thickness in cm	Running Total
1	Calcareous arkose: light gray-red, weathers dark red; fine grained; bedding 2 mm to 20 cm thick, some cross-bedding; quartz, mica, and feldspar grains; ledge former; calcite cement	370	370
2	Conglomerate: clasts 5 mm and less; clasts are sandstone and mudstone; well rounded; weathers red; beds thick and thin along strike	61	431
3	Calcareous arkose: light gray, weathers dark red; fine grained; quartz, mica, and feldspar grains; bedding 2 mm to 20 cm thick, cross-bedding, slope former; calcite cement	91	522
4	Conglomerate: clasts 1 cm and less, sandstone and mudstone; well rounded; weathers red; ledge former	150	762

5	Calcareous arkose: light gray weathers red-brown; medium grained; quartz, abundant mica, feldspar, and mudstone clasts; bedding 2 cm and less thick; mudstone layers between beds weather faster than sands; some organic matter; slope former	732	1404	cross-bedding, graded bedding; medium-grained at bottom to fine grained at top; sparry calcite cement		
6	Conglomerate: clasts 4 cm and less; weathered surface red-brown, some cross-bedded sandstone lenses; lower one-third poorly cemented, upper two-thirds well cemented, ledge former	300	1704	5 Sandy mudstone: dark gray; subangular fine grained quartz, potassium feldspar, plagioclase feldspar, muscovite, biotite, and organic matter; slightly calcareous	15	335
7	Covered, probably sandy shale	640	2344	6 Calcareous arkose: light gray; fine to medium grained; subangular; mineral grains quartz, potassium feldspar, plagioclase feldspar, muscovite, biotite; organic matter, pyrite, and flattened mudstone, sparry calcareous cement with minor silt and clay matrix	124	450
8	Arkosic wacke: light gray-green weathers red-brown, fine grained; quartz, mica, feldspar, and flattened mudstone clasts; organic matter; poorly cemented; slightly calcareous; slope former	61	2405	7 Conglomerate with arkose interbeds: Clasts 2.5 cm and less; clasts flattened mudstone; medium-grained subrounded quartz, potassium feldspar and plagioclase feldspar between clasts and in arkose; organic matter in both; sparry calcite cement in both	134	593
9	Arkosic wacke: light gray-green, weathers red-brown; very fine grained; argillaceous; quartz, mica, and feldspar; flattened mud clasts 3 cm and less; organic matter; bedding 1 cm to 20 cm thick; poorly cemented; slope former	820	3225	8 Calcareous arkose: light gray; coarse grained; subangular quartz, potassium feldspar, plagioclase feldspar, muscovite, and biotite; flattened, well-rounded mudstone clasts 1 mm and less and organic matter; sparry calcite cement surrounding all grains	164	757
10	Calcareous arkose: light gray with dark bands, weathers dark red-brown; fine grained; quartz, abundant mica, and feldspar; organic matter; bedding 4 cm and less thick; some cross-bedding; slope former	760	3985	9 Conglomerate: clasts 6 cm and less; subangular coarse grained quartz, potassium feldspar, plagioclase feldspar, muscovite, and biotite occur between clasts; clasts mudstone; organic matter also found; sparry calcite cement	56	813
11	Calcareous arkose: light gray-green, weathers dark red-brown; fine grained quartz, mica, and feldspar; organic matter; cross-bedded; ledge former, calcareous.	210	4195	10 Sandy mudstone: dark gray; coarse-grained subangular quartz, potassium feldspar, plagioclase feldspar, muscovite, and biotite; clasts and organic matter; calcareous	132	945
12	Mudstone: gray-green, rock fragments 4 cm and less; unit lenses out along strike	30	4225	11 Conglomerate: clasts 5 cm and less; clasts mudstone; some mudstone clasts dark red, others gray; some clasts flattened; coarse grained subangular quartz, potassium feldspar, plagioclase feldspar, muscovite, and biotite; interbedded lenses of very fine-grained arkose with mineral composition same as grains between clasts; organic matter also found; sparry calcite cement	66	1011
13	Calcareous arkose: dark red-brown, same on weathered surface; medium grained; quartz, mica, and feldspar, calcareous cement, ledge former	150	4525	12 Calcareous arkose: light gray; fine grained; subangular; mineral grains quartz, potassium feldspar, plagioclase feldspar, muscovite, and biotite; organic matter in flakes; sparry calcite cement	7	1018
14	Shale with interbedded calcareous arkose: shale dark red, weathers fissile; arkose; dark red weathers same; medium grained; quartz, mica, and feldspar; calcareous cement; slope former	600	5125	Unconformity		
Unit	Core 3	Thickness in cm	Running Total	13 Calcareous arkose: light red; medium grained; subangular; mineral grains quartz, potassium feldspar, plagioclase feldspar, muscovite, and biotite; sparry calcite cement, some stained red	26	1044
1	Calcareous arkose: light gray with dark gray bands; fine grained; subangular; poorly sorted; mineral grains quartz, potassium feldspar, plagioclase feldspar, muscovite, and biotite; organic matter making some dark bands, mudstone composing others; graded bedding, ripple marks, convolute bedding, and cross-bedding; sparry calcite cement	114	114	14 Mudstone: dark red-brown with some white stringers of sparry calcite; wavy bedding	193	1237
2	Sandy mudstone: dark red-brown with gray bands; subangular very fine grained quartz, potassium feldspar, plagioclase feldspar, muscovite, and biotite; organic matter, convolute bedding	26	140	15 Sandy mudstone: dark red-brown with some white stringers of sparry calcite; subangular fine-grained quartz, potassium feldspar, and plagioclase feldspar mineral grains; wavy bedding	66	1308
3	Arkosic wacke: light gray with dark gray bands; very fine grained; subangular; mineral grains quartz, potassium feldspar, plagioclase feldspar, muscovite, and biotite; organic matter, silt, and clay in dark bands; ripple marks; abundant mudstone matrix slightly calcareous; some flattened clasts of mudstone	67	207	16 Sandy limestone: calcite rhombs 0.25 mm and less; fine grained quartz, potassium feldspar, and plagioclase feldspar 20 percent or less of unit; silt and clay around rhombs and grains	41	1344
4	Calcareous arkose: light gray with dark gray bands; fine to medium grained; subangular; poorly sorted; mineral grains quartz, potassium feldspar, plagioclase feldspar, muscovite, and biotite; organic matter and pyrite abundant in dark bands which have silt and clay matrix; dark bands; minor	113	320	17 Sandy calcareous mudstone: light red-brown; subangular fine grained quartz, potassium feldspar, and plagioclase feldspar mineral grains; sparry calcite cement	6	1350

18	Calcareous arkose: dark red-brown with white patches; medium grained; subangular; mineral grains quartz, potassium feldspar, plagioclase feldspar; sparry calcite cement	355	1705	12	Conglomerate with thin sandstone lenses: conglomerate clasts 2 cm and less; clasts composed of mudstone, rounded; graded bedding; calcareous mud matrix; sandstone lenses medium grained; light red; grains quartz, potassium feldspar, and plagioclase feldspar; sparry calcite cement	128	1364
Unit	Core 9	Thickness in cm	Running Total				
1	Conglomerate and mudstone interbedded: conglomerate-mudstone ratio 1:1; average bed thickness 20 cm for both rock types; mudstone; dark gray with light bands; organic matter present; calcareous; bedding uneven, some load structures; some beds disintegrated in a form much like pencil shale; conglomerate; clasts 3 cm and less, composed of rounded and flat pebble mudstone; mineral grains between clasts quartz, potassium feldspar, and plagioclase feldspar; grain size medium to coarse grained, sparry calcite cement	319	319	13	Calcareous mudstone: mottled red and yellow-green; flattened mudstone intraclasts.	61	1425
2	Arkosic wacke: very fine grained; dark and light red bands; mineral grains quartz, potassium feldspar, plagioclase feldspar, and muscovite; bedding types horizontal cross-bedding; calcareous silt and clay matrix	33	352	14	Conglomerate: light gray; clasts 4 mm and less, well rounded, mudstone; quartz, chert, potassium feldspar, plagioclase feldspar, muscovite, and biotite between clasts; organic matter present; sparry calcite cement; mudstone clasts flattened, some dark red	117	1541
3	Conglomerate: clasts 4 cm and less composed of mudstone; mineral grains of quartz, potassium feldspar, biotite, and muscovite between clasts; sparry calcite cement	50	402	15	Arkosic wacke: banded light red and gray; fine to very fine grained; grains are quartz, potassium feldspar, and plagioclase feldspar; cross-bedding and uneven bedding; silt and clay matrix	66	1608
4	Arkosic wacke: light gray; very fine grained; subangular; grains of quartz, potassium feldspar, plagioclase feldspar, biotite, muscovite, and chlorite; organic matter concentrated in thin bands; cross-bedding; calcareous silt and clay matrix; some ripple marks	249	696	16	Mudstone with interbedded arkosic wacke: Mudstone arkosic wacke ratio 4:1; mudstone dark red, calcareous; arkosic wackes light gray; fine to very fine grained; mineral grains quartz, potassium feldspar, and plagioclase feldspar; calcareous silt and clay matrix	83	1691
5	Arkosic wacke and mudstone; dark gray; fine grained; arkosic wacke, stones in thin 5 cm or less alternating beds; mudstone dominating; bands composed of quartz, potassium feldspar, and plagioclase; calcareous	85	781	17	Conglomerate: clasts 3 cm and less, composed of mudstone; quartz, potassium feldspar, and plagioclase feldspar grains between clasts; sparry calcite cement	60	1751
6	Arkosic wacke: light gray; medium grained; grains of quartz, potassium feldspar, plagioclase feldspar, mud clasts, biotite, and muscovite; some thin claystone bands; minor cross-bedding; calcareous mud matrix	185	966	18	Sandy mudstone: dark red; sand grains composed of quartz, potassium feldspar, and plagioclase feldspar; mudstone like a pencil shale.	23	1774
7	Calcareous arkose and conglomerate interbedded: conglomerate-sandstone ratio 3:1; clasts 3 cm and less, composed of mudstone; sandstones medium grained; grains of quartz, potassium feldspar, and plagioclase feldspar; sparry calcite cement	35	1001	19	Conglomerate: clasts 2 cm and less, composed of mudstone; medium-grained quartz, potassium feldspar, and plagioclase feldspar between clasts; sparry calcite cement	4	1778
8	Conglomerate: clasts 2 cm and less, composed of mudstone, well rounded; quartz, potassium feldspar, and plagioclase feldspar grains between clasts; coarse grained; subangular; differential compaction shown; cross-bedding; some organic matter and pyrite; sparry calcite cement.	149	1150	20	Arkosic wacke: light red and gray; very fine grained; grains quartz, potassium feldspar, plagioclase feldspar, muscovite, biotite, and chlorite; calcareous silt and clay matrix	107	1885
9	Calcareous arkose: light gray; medium grained; subangular; grains of quartz, potassium feldspar, plagioclase feldspar, and minor mica; sparry calcite cement	12	1162	21	Conglomerate and calcareous arkose with small mudstone lenses: conglomerate clasts 1 cm and less; clasts composed of mudstone flattened; medium-grained quartz, potassium feldspar, and plagioclase feldspar grains between clasts; sparry calcite cement; calcareous arkose medium grained, red and light gray; quartz, potassium feldspar, and plagioclase feldspar; calcareous cement	59	1944
10	Conglomerate: clasts 5 cm and less, of mudstone; medium-grained quartz, potassium feldspar, plagioclase feldspar between clasts; sparry calcite cement	51	1213	Unconformity			
11	Calcareous arkose: light gray; coarse grained; subangular; mineral grains of quartz, potassium feldspar, plagioclase feldspar, muscovite, and biotite; cross-bedding; sparry calcite cement	23	1236	22	Calcareous arkose: dark red with white patches; medium grained; subangular; grains quartz, potassium feldspar, and plagioclase feldspar, calcareous cement with red stain	238	2182
				23	Core missing	60	2242

## REFERENCES CITED

- Clair, J. R., 1958, Subsurface stratigraphy of the Paradox Basin (Colorado Plateau): Rocky Mtn. Assoc. Geol., Symposium on Pennsylvanian rocks of Colorado and adjacent areas, p. 31-46.
- Keller, W. D., 1953, Illite and montmorillonite in green sedimentary rock: Jour. Sed. Petrol., v. 23, p. 3-9.
- Kelley, V. C., 1955, Regional tectonics of the Colorado Plateau and relationship to the origin and distribution of uranium: Univ. New Mexico Publ. in Geol., v. 5, 120 p.
- Lekas, M. A., and Dahl, H. M., 1956, The geology and uranium deposits of the Lisbon Valley anticline, San Juan County, Utah: Intermountain Assoc. Petrol. Geol., 7th Field Conf., p. 161-68.

- Pettijohn, F. J., 1975, *Sedimentary rock*, 3rd ed.: Harper and Row, New York, 682 p.
- Roebeck, R. C., 1958, Chinle and Moenkopi formations, southeastern Utah: Intermountain Assoc. Petrol. Geol., 9th Field Conf., p. 169-71.
- Stewart, J. H., Poole, F. G., and Wilson, R. F., 1972, Stratigraphy and origin of the Chinle Formation and related Upper Triassic strata in the Colorado Plateau region with a section on sedimentary petrology by R. A. Cadigan and a section on conglomerate studies by W. Thordorson, H. F. Albbe, and J. H. Stewart: U.S. Geol. Surv. Prof. Paper 690, 336 p.
- Weir, G. W., 1955a, Lisbon Valley area, Utah-Colorado: U.S. Geol. Surv. Rpt. TEI-590, p. 39-42.
- , 1955b, Lisbon Valley area, Utah-Colorado: U.S. Geol. Surv. Rpt. TEI-540, p. 50-51.
- , 1956, Lisbon Valley, Utah-Colorado: U.S. Geol. Surv. Rpt. TEI-640, p. 51-58.
- , 1958, Lisbon Valley area, Utah-Colorado: U.S. Geol. Surv. Rpt. TEI-750, p. 14-25.
- Weir, G. W., and Puffett, W. P., 1959, Lisbon Valley, Utah-Colorado: U.S. Geol. Surv. Rpt. TEI-751, p. 9-13.
- Weir, G. W., Puffett, W. P., and Kennedy, V. C., 1957a, Lisbon Valley, Utah-Colorado, U.S. Geol. Surv. Rpt. TEI-700, p. 36-46.
- , 1957b, Lisbon Valley, Utah-Colorado: U.S. Geol. Surv. Rpt. TEI-690, v. 1, p. 95-103.
- Wengerd, S. A., and Matheny, M. L., 1958, Pennsylvanian System of Four Corners region: Bull. Amer. Assoc. Petrol. Geol., v. 42, p. 2048-2106.
- Wright, J. R., and Dickey, D. D., 1958, Pre-Morrison Jurassic strata of southeastern Utah: Intermountain Assoc. Petrol. Geol., 9th Field Conf., p. 172-81.